



Quantifying the influence of wood carbon fractions on tree- and forest ecosystem-scale carbon estimation in a temperate forest

Adam R. Martin ¹, Dilene Mugenzi ¹, Sean C. Thomas ⁶, Audrey Barker-Plotkin ², Mahendra Doraisami ¹, Mark Givelas ¹, Adam Gorgolewski ³, Rachel O. Mariani ¹, David Orwig ², Benton N. Taylor ^{4,5}, Leeladarshini Sujeeun ¹

¹ Department of Physical and Environmental Sciences, University of Toronto Scarborough, Scarborough, ON, Canada.

² Harvard Forest, Harvard University, Petersham, Massachusetts, USA

³ Haliburton Forest Research Institute, Haliburton Forest and Wild Life Reserve Ltd., 1095 Redkenn Rd., Haliburton, ON, Canada.

⁴ Department of Organismic and Evolutionary Biology, Harvard University, Cambridge, Massachusetts, USA

⁵ The Arnold Arboretum of Harvard University, Roslindale, Massachusetts, USA

⁶ Institute of Forestry and Conservation, Daniels Faculty of Architecture, Landscape, and Design, University of Toronto, Toronto, ON, Canada.

Correspondence to: adam.martin@utoronto.ca

Abstract. Accurate forest carbon (C) accounting is critical for understanding the role forests play in the global C cycle. Forest C accounting relies on wood carbon fractions (CF) in order to convert estimates of tree biomass into C stock estimates, which are then upscaled to estimate forest C stocks at larger spatial scales. Generic wood CFs are often used in C accounting frameworks, despite evidence suggesting this trait varies widely across species, and that this variability influences our understanding of C stocks in trees and forests. Here, we couple data from over 39,000 trees in a 13.5-ha forest dynamics plot in central Ontario, Canada, with open-access wood CF databases, to quantify how wood CFs influence C stock estimates at individual tree- through to 400 m² and 1-ha forest ecosystem scales. In comparison to generalized wood CF assumptions (e.g., assuming a 50% CF or using wood CFs from the Intergovernmental Panel on Climate Change), species-specific wood CFs significantly influence C estimates at multiple scales. In comparison to species-specific wood CF data, tree-level estimates derived from other wood CF assumptions were biased by 0.8-3.9 kg of C per tree on average, with differences ranging up to >500 kg of C in large trees. While relatively small, these tree-level differences compound at larger spatial scales, with C stocks estimated using generalized wood CFs differing by 1.3-3.2 Mg of C ha⁻¹ on average vs. those generated using species-specific wood CFs. These forest-scale discrepancies in C estimates increase in forest stands with high amounts of aboveground biomass in large trees and greater proportions of gymnosperms, in some instances exceeding 23.5 Mg of C ha⁻¹ in especially biomass-dense gymnosperm-dominated forest stands. When extrapolated to the temperate forest biome, our results indicate that a 50% wood CF assumption—historically and presently one of the most common methodological assumptions in forest C research—overestimates global C stocks by 2.2-2.5 Pg of C. Our study is among the first to examine how wood CF assumptions influence tree- and forest-scale C accounting. We specifically demonstrate that species-specific wood CF data—especially for species that comprise the largest trees—are critical to ensuring accurate C stock estimates derived from forest and tree inventory data.



37 1 Introduction

38 Forests play a critical role in the global carbon (C) cycle and in mitigating climate change, with estimates
 39 from 2020 indicating that forest biomes store $\sim 870 \pm 61$ Pg of C globally, of which ~ 135.78 Pg ($\sim 15\%$) originate in the
 40 temperate forest biome (Pan et al., 2024). Between 1990–2010, forests across the globe sequestered $\sim 3.6 \pm 0.4$ Pg C
 41 year⁻¹ (Pan et al., 2024). While global forest C sequestration has remained stable at this rate over the past three decades,
 42 the differential impacts of biotic and abiotic environmental change drivers on forest structure and composition across
 43 space and time (e.g., Anderegg et al., 2015; Hartmann et al., 2022; Simler-Williamson et al., 2019; Hogan et al., 2024;
 44 Weed et al., 2013) have led to distinct changes in sink strength across and within biomes (Yang et al., 2023; Harris et
 45 al., 2021; Xu et al., 2021).

46 Specifically, the C sinks in both boreal and tropical intact forests have declined by an estimated 36% and
 47 31%, respectively, while temperate forest C sinks have increased by an estimated 30% since 1990, from 0.53 ± 0.04 Pg
 48 C year⁻¹ in the 1990s to 0.69 ± 0.05 Pg C year⁻¹ in the 2010s. Increasing C sink strength among temperate forests was
 49 largely driven by afforestation in China, which offset reductions in temperate forest C sink strength in the United
 50 States and Europe (Pan et al., 2024). Standing carbon stock densities in temperate forests have followed similar trends,
 51 increasing from 157.03 Mg C ha⁻¹ in the 1990s to 171.00 Mg C ha⁻¹ through the 2010s (Pan et al., 2024).

52 Within temperate forests, $\sim 38\%$ of C stocks persist as living aboveground biomass (AGB)—the focus of our
 53 research here—while 54% is present in soils: values that closely approximate global estimates where 43% of C stocks
 54 exist within living AGB and $\sim 45\%$ in soils (with $\sim 8\%$ in deadwood and $\sim 4\%$ in leaf litter) (Pan et al., 2024). Carbon
 55 stocks and fluxes in living AGB in temperate forests, especially in North America, therefore represent a vitally
 56 important component of current and future global forest C cycles (Domke et al., 2020; Yang et al., 2023). In turn,
 57 accurate estimates of temperate tree and forest C stocks are critical for understanding the role forests play in mitigating
 58 the climate forcing potential of anthropogenic greenhouse gas emissions.

59 Obtaining tree- and forest-level C estimates entails first determining AGB, generally done through field-
 60 based forest surveys (e.g., Davies et al., 2021) or remote sensing methods (e.g., Coops et al., 2021), and then
 61 converting AGB to C stocks by multiplying AGB by a wood carbon fraction (CF) that represents the proportion of
 62 biomass comprised of elemental carbon (Martin and Thomas, 2011; Thomas and Martin, 2012). In forest C estimation
 63 studies and models, researchers commonly assume generic wood CFs, with 50% being the most common assumption
 64 or other generic wood CF values (reviewed by Martin et al., 2018). However, recent studies have demonstrated that a
 65 single wood CF conversion factor may overlook ecologically meaningful variability in wood chemistry across species,
 66 ultimately leading to inaccurate estimates of tree- and forest-scale C stocks.

67 Meta-analyses have shown that wood CFs vary across all tree species and forested biomes, ranging from 28-
 68 65% (Doraisami et al., 2022 and references therein). Databases of wood CFs indicate that temperate tree species have
 69 CFs ranging from 40.5–55.6%, with angiosperms ($46.5 \pm 0.3\%$ [s.e.]) typically having lower average CFs than
 70 gymnosperms ($50.1 \pm 0.4\%$ [s.e.]). These trends are hypothesized to reflect a larger contribution of C-rich lignin to
 71 wood chemical composition in gymnosperms, and generally lower lignin/holocellulose ratios in angiosperm wood
 72 (Doraisami et al., 2024; Martin et al., 2018; Lamblom and Savidge, 2003). Furthermore, the published literature
 73 suggests that using a 50% wood CF assumption, or other CFs recommended by the Intergovernmental Panel on



74 Climate Change (IPCC), systematically overestimate temperate forest C stocks (cf. Table 1 in Martin et al., 2018).
 75 However, we lack a precise understanding of how this error at the tree level (in terms of kg of C tree⁻¹) scales up to
 76 the ecosystem level (in terms of Mg C ha⁻¹ of forest), since mean CF values across tree species do not correspond to
 77 mean values representative of whole ecosystems.

78 The literature documenting variability in wood chemical traits suggests C accounting errors associated with
 79 generic wood CF assumptions (especially a 50% assumption) may be lower in certain forest communities compared
 80 to others, due to varying species composition and the proportion of angiosperms and gymnosperms. Specifically, in
 81 forests dominated by gymnosperms, one might expect lower C accounting errors, since gymnosperm CFs are closer
 82 to 50% or existing IPCC recommendations, as compared to angiosperms (Doraisami et al., 2024; Martin et al., 2018;
 83 Lamblom and Savidge, 2003). Conversely, C accounting in angiosperm-dominated forests would be expected to be
 84 overestimated by generic wood CF assumptions. To our knowledge, no study has integrated forest inventory data with
 85 wood CF data to test this hypothesis or quantify the magnitude of large-scale biases.

86 Recently published frameworks exist for selecting appropriate wood CFs for forest C accounting studies and
 87 models under different data availability scenarios (Doraisami et al., 2024). Specifically, recent work suggests that
 88 there exist different options for wood CF values that can be applied to C accounting methods and models. Generally,
 89 among the levels of wood CF determination, species-specific wood CFs—derived from wood chemical trait data
 90 (Lamblom and Savidge, 2003) or trait databases (Doraisami et al., 2022)—should produce tree- and ultimately forest-
 91 level C estimates that account for species differences in wood C chemistry. The level of species-specificity in wood
 92 CFs is considered the most data-informed trait option, relative to other wood CFs that are A) generalized for
 93 gymnosperms and angiosperms at varying levels of biome-specificity, or B) reflect a generic 50% wood CF
 94 assumption (Doraisami et al., 2024). Explicitly comparing how estimates of C differ across these approaches, across
 95 tree- to forest ecosystem scales, would provide a more detailed understanding of the degree to which wood CF
 96 assumptions influence our understanding of temperate (and global) forest C dynamics.

97 In this study, we paired forest inventory data from a large-scale temperate research plot (Davies et al., 2021;
 98 Kish et al., 2022) with CFs obtained from open-access wood CF databases (Doraisami et al., 2022) and recently
 99 developed decision matrices for integrating wood CFs into C accounting protocols (Doraisami et al., 2024), to
 100 characterize the role that wood CF variation plays in forest C accounting. We integrated these to address the following
 101 research questions: 1) What is the magnitude of error in tree-level C stocks associated with generic wood CF
 102 assumptions? 2) How does this error scale up from the tree level to the forest ecosystem level? 3) Does the magnitude
 103 of this error vary according to forest attributes, including tree species composition and/ or forest biomass?

104

105 **2 Materials and Methods**

106 *2.1 Study site*

107 Our study was conducted in the Haliburton Forest Dynamics Plot (HFDP), in the Haliburton Forest & Wild
 108 Life Reserve Ltd., in Ontario, Canada (43° 130' N, 78° 350' W) (Fig. 1). The HFDP is among a network of forest
 109 inventory plots of the Forest Global Earth Observatory (ForestGEO): a network comprised of 71 forest inventory plots
 110 located across all forested biomes and ranging in size from 4-50 ha (Davies et al., 2021). Across all ForestGEO plots,



every tree ≥ 1 cm diameter at breast height (DBH) has its DBH measured, is identified to species, and is mapped every five years (Davies et al., 2021). The HFDP is located in the temperate forest biome and is representative of the Great Lakes–St. Lawrence forest region of eastern Canada and the United States (Kish et al., 2022).

The HFDP is a 13.5 ha forest inventory plot situated on the margins of a freshwater lake and has an average elevation of 434 m a.s.l. across a gradient ranging from 413–454 m a.s.l (Fig. 1). The HFDP consists of trees belonging to 30 species, with *Acer saccharum* (L.), *Abies balsamea* ([L.] Mill.), *Fagus grandifolia* (Ehrh.), and *Tsuga canadensis* (L.) being among the most common and dominant canopy species. Within the HFDP, other common angiosperm species include *Acer rubrum* (L.), *Betula allegheniensis* (Britt.), *Betula cordifolia* (Regel), *Prunus serotina* (Ehrh.), and *Quercus rubra* (L.), while other common gymnosperms include *Picea glauca* ([Moench] Voss), *Pinus strobus* (L.), and *Thuja occidentalis* (L.) (Kish et al., 2022). Shrubs that reach ≥ 1 cm DBH in the HFDP are also included in the census and our analysis here. In recent years, forest structure and C dynamics have been especially influenced by the presence and spread of beech bark disease, which is currently among the most important drivers of biomass and C dynamics in the HFDP (Kish et al., 2022).

2.2 Tree-level aboveground biomass and carbon estimation

Based on the ForestGEO sampling protocols (Davies et al., 2021), we used stem DBH values taken from the 2014 HFDP recensus to quantify aboveground biomass (AGB) and C stocks for $n=39,064$ trees ≥ 1 cm DBH, while assuming five different wood CF scenarios. To do so, we first used DBH measurements in conjunction with published species-specific allometric equations to derive tree-level AGB estimates. Specifically, we employed allometric equations published by Lambert et al. (2005), which estimates AGB (in kg) for three separate tree compartments—stems, branches, and bark—as:

$$y_{\text{wood}} = \beta_{\text{wood1}} \text{DBH}^{\beta_{\text{wood2}}} \quad (\text{Equation 1})$$

$$y_{\text{branches}} = \beta_{\text{branches1}} \text{DBH}^{\beta_{\text{branches2}}} \quad (\text{Equation 2})$$

$$y_{\text{bark}} = \beta_{\text{bark1}} \text{DBH}^{\beta_{\text{bark2}}} \quad (\text{Equation 3})$$

where tree DBH is measured in cm, β_{wood1} and β_{wood2} represent species-specific model coefficients for estimating AGB in stem wood, $\beta_{\text{branches1}}$ and $\beta_{\text{branches2}}$ represent species-specific model coefficients for estimating AGB in branches, and β_{bark1} and β_{bark2} represent species-specific model coefficients for estimating AGB in bark (Lambert et al., 2011). Based on these values, we then estimated total AGB for each tree (y_{total}) as:

$$y_{\text{total}} = y_{\text{wood}} + y_{\text{branches}} + y_{\text{bark}} \quad (\text{Equation 4})$$

Tree-level C estimates were then calculated based on AGB data (from Equation 4), using varying degrees of wood CF specificity: low degrees of specificity entail wood CFs that are more general in nature (i.e., a 50% wood CF assumption for all trees), whereas a high degree of specificity entails (for example) wood CFs that are informed by species-specific trait data. The wood CFs employed in our study broadly correspond to Tiers 1–3 forest C stock estimation methods employed by the IPCC, which incorporate wood CFs at five different levels based on the framework published by Doraisami et al. (2024).



Tree-level C estimates at Level 1 (C_{tree1}) entail the use of species-specific wood CFs based on stem tissue. The use of wood CFs of stem tissue is due to its close correlation with wood C concentrations from all plant tissues within a given species (Martin et al., 2018; Thomas and Martin, 2012), especially with respect to species in the HFDP (Martin et al., 2015). Level 2 (C_{tree2}) presents a lower degree of species-specificity, whereby wood CFs are specific to angiosperms (46.5%) and gymnosperms (50.1%) from temperate forested biomes. Level 3 (C_{tree3}) uses taxonomic divisions; however, the values for angiosperms (46.8%) and gymnosperms (48.5%) are more generalized as they are derived from data for trees across all forested biomes. Wood CFs employed to generate values of C_{tree2} and C_{tree3} are based on global analyses of wood CF data (Martin et al., 2018) from open-access databases (Doraisami et al., 2022), which have specifically been proposed as alternatives to existing IPCC-based forest C accounting protocols (Doraisami et al., 2024). The most generalized two levels, Levels 4 and 5, both apply a single conversion factor when converting AGB to carbon. Specifically, Level 4 (C_{tree4}) is based on IPCC forest C accounting guidelines (Ipcc, 2006), which employs a single default wood CF of 0.47 for all trees. Lastly, Level 5 (C_{tree5}) entails the use of the coarsest (and most common) wood CF assumption, employing a default wood CF of 50% for all trees. In summary, for each of the $n=39,064$ individual trees within the HFDP, we generated five different tree-level C values denoted as C_{tree1} through C_{tree5} , with decreasing species-specificity in their wood CFs used to convert all values of y_{total} into C_{tree} values.

162

2.3 Statistical analysis—the influence of wood CFs on tree-level C estimates

All analyses were performed using R v. 4.2.2 statistical software (R Foundation for Statistical Computing, Vienna, Austria). First, we performed paired t -tests to assess differences in \log_{10} -transformed C_{tree} values across different wood CF assumptions ($n=39,064$ trees in all paired t -tests, implemented using the ‘t.test’ function). Here, C_{tree1} , which represents our most species-specific wood CF assumption, was taken as a reference point such that only the following contrasts were assessed: C_{tree1} vs. C_{tree2} ; C_{tree1} vs. C_{tree3} ; C_{tree1} vs. C_{tree4} ; and C_{tree1} vs. C_{tree5} . We refined our analysis to these contrasts only because we were explicitly interested in understanding how species-specific wood CFs refined our understanding of tree- and forest-level C stocks compared to more generalized wood CF assumptions.

We then conducted more detailed analyses of differences in C estimates (measured in kg C tree^{-1}) across the same wood CF contrasts (i.e., C_{tree1} vs. C_{tree2} – C_{tree5}) for all $n=39,064$ trees in our dataset. Differences in tree-level C estimates (measured in kg C tree^{-1}) were calculated as C_{tree1} minus C_{tree2} – C_{tree5} , such that negative values denote instances where more generalized wood CFs overestimate tree-level C estimates (compared to species-specific wood CFs) and positive differences denote instances where generic wood CFs underestimate tree-level C estimates (compared to species-specific wood CFs assumptions).

Lastly, we used analysis of covariance (ANCOVA) to test if differences in tree-level C estimates owing to wood CF assumptions differ across taxonomic divisions and/or scale with tree DBH. These models were fit for each of the four sets of differences (i.e., C_{tree1} minus C_{tree2} – C_{tree5}), where differences in tree-level C estimates were predicted as a function of an intercept term (corresponding to an average C stock difference between C_{tree1} vs. the



other four C_{tree} estimates), taxonomic division (as a categorical factor), DBH, a second-order polynomial DBH term (DBH^2), as well as division-by-DBH and division-by- DBH^2 interaction terms.

2.4 Statistical analysis—the influence of wood CFs on forest-level C estimates

To assess how wood CF assumptions scale from trees to forests, we used our data to scale all five C_{tree} values to two area-based estimates: 1) a 20-by-20 m subplot level (C_{subplot}) and 2) a per ha level (C_{ha}) (Fig. 1). At both scales, we again derived five distinct values of C_{subplot} and C_{ha} for each wood CF assumption (also denoted as $C_{\text{subplot}1}$ through $C_{\text{subplot}5}$, and $C_{\text{ha}1}$ through $C_{\text{ha}5}$). In the HFDP, there are $n=369$ distinct subplots, which were then aggregated into $n=10$ ha of forest following previous analyses of deadwood C dynamics in the HFDP (Doraisami et al, unpublished). Due to the irregular shape of the HFDP, all C_{subplot} values derived from subplots situated on the lake margin were scaled to their respective area (Fig. 1), with a number of subplots omitted from analyses of C_{ha} data.

At both scales, we again calculated differences in C_{subplot} and C_{ha} values, specifically comparing values underpinned by species-specific wood CF data ($C_{\text{subplot}1}$ and $C_{\text{ha}1}$, respectively) vs. values derived from more general wood CFs ($C_{\text{subplot}2}$ through $C_{\text{subplot}4}$, and $C_{\text{ha}1}$ through $C_{\text{ha}4}$, respectively). We then used ANCOVA models to evaluate how tree biomass and species composition at the subplot or ha scale influenced differences in C_{subplot} or C_{ha} values. Here, we were especially interested in understanding the role that large trees play in C estimate differences (akin to our DBH terms in the tree-level ANCOVA models above), and the role that species composition may play in driving differences (akin to the taxonomic division model terms in the ANCOVAs described above). Therefore, in these models, differences in C_{subplot} or C_{ha} values between any two estimates were predicted as a function of large tree biomass (defined as the total kg of biomass in trees ≥ 10 cm DBH in a subplot or per ha), small tree (1-10 cm DBH) biomass, and the proportion of biomass represented by gymnosperms in a subplot or per ha. To allow for non-linearity in relationships between biomass and discrepancies in C estimates (as informed by our tree-level analysis described below), we also included 2nd-order polynomial terms in these models for large tree biomass and small tree biomass. The sample sizes for these models were $n=368$ subplots and $n=10$ ha; so, we interpret the per ha analysis cautiously. Finally, these models did not include any biomass-by-composition interaction terms to simplify the interpretation of our results and avoid model over-fitting (especially at the per ha scale of analysis).

3. Results

3.1 The influence of wood CF assumptions on tree-level C estimates

Wood CF assumptions influenced tree-level C stock estimates, with estimates of $C_{\text{tree}1}$ generated using species-specific wood CFs differing significantly from all other C_{tree} estimates (paired t -test on \log_{10} -transformed data, $p < 0.001$, absolute $t_{39,063} \geq 255.9$ in all four comparisons; Tables 1 and 2). In all but the instance of a 50% wood CF assumption ($C_{\text{tree}5}$), species-specific wood CFs ($C_{\text{tree}1}$) resulted in significantly higher average tree-level C estimates (mean=69.7 kg, median=2.35 kg, range=0.045-7783.82 kg) vs. those generated using: A) wood CFs for temperate biome trees specific to gymnosperms and angiosperms ($C_{\text{tree}2}$, mean=68.9 kg, median=2.28 kg, range=0.044-7,799.39 kg); B) non-biome-specific wood CFs for gymnosperms and angiosperms ($C_{\text{tree}3}$, mean=67.59 kg, median=2.3 kg,



range=0.044-7,550.31 kg); and C) the IPCC default wood CF assumption (C_{tree4} , mean=65.9 kg, median=2.27 kg, range=0.044-7,270.09 kg). A 50% wood CF assumption (C_{tree5}) resulted in considerably higher tree-level C values (mean=70.56 kg, median=2.43 kg, range=0.047-7,783.82 kg) (Table 1).

Differences in C_{tree1} vs. other C_{tree} estimates varied significantly as a function of taxonomic division and DBH (ANCOVA model $r^2=0.266-0.971$, $p<0.01$ in all cases; Fig. 2, Table A1). The ANCOVA also returned statistically significant terms for DBH^2 , and the division-by-DBH and division-by- DBH^2 interaction terms ($p<0.01$ in all but one case where $p=0.048$): differences between C_{tree1} and other C_{tree} estimates were larger in gymnosperms vs. angiosperms ($p<0.01$ for the taxonomic division and division-by-DBH interaction terms) and scaled non-linearly with tree size ($p<0.01$ for the taxonomic division and division-by- DBH^2 interaction terms; Fig. 2, Table A1). Non-linear increases in the absolute differences between C_{tree1} vs. $C_{tree2-5}$ largely tracked allometric relationships associated with different tree species, such that these differences in C_{tree} increased with tree-level AGB (i.e., y_{total} values). The rate at which C_{tree} differences increased with DBH depended on species identities (Fig. 2), reflecting differences in allometric relationships between y_{total} and DBH. The strong influence of DBH on tree-level C estimates is also evidenced by our results showing that the lower 5% of tree-level C estimates was largely consistent across C_{tree1} through C_{tree5} (range of lower 5% confidence intervals [CI]=0.11-0.119 kg C), though differences were more pronounced at the upper 90% CI ($C_{tree1}=169.69$ kg C vs. $C_{tree2-Ctree5}=160.08-171.37$ kg C) and upper 95% CI ($C_{tree1}=370.58$ kg C vs. $C_{tree2-Ctree5}=352.59-377.508$) (Fig. 2, Table 2).

3.2 The influence of wood CF assumptions on forest-level C estimates at small spatial scales

Differences in tree-level C estimates ($C_{tree1}-C_{tree5}$) scaled up to influence forest-level C stocks at both the 400- m^2 subplot ($C_{subplot1}-C_{subplot5}$) and ha ($C_{ha1}-C_{ha5}$) scales. At the subplot level, C stock estimates derived from species-specific wood CFs ($C_{subplot1}$) differed significantly from all other C stock estimates (paired t -test $p<0.001$, absolute $t_{39,063}\geq 24.1$ in all four comparisons; Fig. 3, Table 2, Fig. A1). Mean $C_{subplot}$ values owing to different wood CF assumptions ranged from 6,995-7,489 kg C 400 m^2 (median range of $C_{subplot}$ values=4,278-4,580 Mg C 400 m^2). At this scale of analysis, the most generalized wood CF assumptions led to the widest range of average $C_{subplot}$ values, with the IPCC-recommended wood CF ($C_{subplot4}$) resulting in the lowest mean/median $C_{subplot}$ estimates, and a 50% wood CF ($C_{subplot5}$) resulting the highest mean/median estimates (Table 2).

Consistent with the previous findings of variability in C_{tree} estimates being especially pronounced in large trees, statistically significant differences in $C_{subplot1}$ vs. all other $C_{subplot}$ estimates were also driven by high-biomass subplots. Specifically, the lower 5th percentile of $C_{subplot}$ ranged by 87 kg of C, and the higher 95th percentile of $C_{subplot}$ values across all estimates ranged by over 468 kg of C (Table 2). An ANCOVA model predicting differences in $C_{subplot}$ as a function of subplot-level characteristics corroborated this trend, indicating that differences in $C_{subplot1}$ values vs. $C_{subplot2}-C_{subplot5}$ values were statistically correlated with the amount of subplot biomass contained in large trees ($p<0.01$, partial $r^2=0.221-0.961$ for the large tree biomass term; Fig. 3, Table A2). However, the wide range of partial r^2 values for the large tree biomass term indicates that these relationships were idiosyncratic.

Differences between $C_{subplot1}$ vs. $C_{subplot3}$ (taxonomic division-specific wood CFs) and $C_{subplot4}$ (IPCC-recommended wood CFs) were consistently positive, with differences ranging from 0.6-2,927.7 kg of C per subplot



(mean difference=223.9 and 402.9 kg of C per subplot, respectively), indicating that these assumptions consistently underestimate C_{subplot} values compared to species-specific wood CF data (Fig. 3). Differences in C_{subplot1} vs. C_{subplot3} and C_{subplot4} became larger as the amount of total biomass contained in large trees increased (ANCOVA model parameter $p < 0.01$, partial $r^2 = 0.932$ and 0.961 , respectively, Table A2). This trend indicates that underestimates in C_{subplot3} and C_{subplot4} values (compared to C_{subplot1} estimates) increase with greater subplot-level biomass. In these comparisons, we also found a statistically significant contribution of gymnosperm biomass proportion explaining these differences (ANCOVA model parameter $p < 0.01$, partial $r^2 = 0.087$ and 0.635 , respectively, Table A2).

Comparatively, differences in C_{subplot1} vs. C_{subplot2} (i.e., biome-specific wood CFs for angiosperms and gymnosperms) were smaller (mean difference=85.5 kg C subplot⁻¹, range=-29.7 to 225.9 kg C subplot⁻¹) and were both positive and negative, indicating that the wood CF assumptions embedded in C_{subplot2} led to both over- and underestimates of C_{subplot} compared to estimates using species-specific data. Here, differences in C_{subplot} estimates were more strongly dictated by species composition, such that gymnosperm biomass proportion was the strongest correlate of these C_{subplot1} vs. C_{subplot2} differences (ANCOVA model parameter $p < 0.01$, partial $r^2 = 0.654$ and 0.635 , respectively, Table A2). Large tree biomass played a secondary, albeit statistically significant, role in governing C_{subplot} estimation differences (ANCOVA model parameter $p < 0.01$, partial $r^2 = 0.087$ and 0.635 , respectively), and these relationships were non-linear (Fig. 3).

Differences between C_{subplot1} and C_{subplot5} (a 50% wood CF fraction) were unique in that these differences were the only negative average values (mean difference=-91.5 kg C subplot⁻¹), indicating that a 50% assumption overestimates C_{subplot} values. However, individual differences calculated for C_{subplot1} vs. C_{subplot5} did indicate that a 50% wood CF assumption resulted in both over- and underestimates compared to species-specific wood CF data. The 50% wood CF overestimated C_{subplot} values in 342 of 368 subplots, with these overestimates being much larger than the few underestimates (Fig. A1). Again, in these comparisons, species composition was the strongest correlate of these differences: as gymnosperm proportions increased, the differences between C_{subplot} values generated using species-specific data vs. a 50% assumption generally grew closer to 0 (ANCOVA model parameter $p < 0.01$, partial $r^2 = 0.635$, respectively; Table A2). The amount of biomass in large trees also influenced this relationship, albeit in a non-linear manner (Fig. 3). Here, trends indicated that as large gymnosperm biomass increased, differences in C_{subplot1} vs. C_{subplot5} became less negative; conversely, differences in C_{subplot1} vs. C_{subplot5} values were largest in subplots with high angiosperm proportions (Fig. 3).

3.3 The influence of wood CF assumptions on forest-level C estimates at larger spatial scales

Species-specific wood CFs led to higher forest C stocks on a per ha scale (C_{ha1}) and resulted in statistically higher estimates than those based on more generalized wood CFs (namely, $C_{\text{ha2-C}_{\text{ha4}}}$; $t_9 \geq 5.8$, $p < 0.01$ in all three paired t -tests; Fig. 4, Fig. A2, Tables 1 and 2). Specifically, in these comparisons, C_{ha1} averaged 83.3 Mg C ha⁻¹, vs. 80.1-80.6 Mg C ha⁻¹ on average under $C_{\text{ha2-C}_{\text{ha4}}}$ assumptions (Table 1). Similar to our tree- or subplot-level analyses, statistically significant differences across C_{ha1} vs. other estimates were most pronounced at the higher range of C_{ha} values (Table 2). Furthermore, across these comparisons (C_{ha1} vs. $C_{\text{ha2-C}_{\text{ha4}}}$), species-specific wood CF data increased C_{ha} estimates by 2.6-9.0 Mg C ha⁻¹ on average, with differences ranging from 1.3-23.5 Mg C ha⁻¹ (Fig. 4). Differences



in C_{ha} values mostly increased as wood CF assumptions became more generalized, being most pronounced when comparing C_{ha1} to estimates generated using the IPCC's default value (C_{ha4} ; Fig. 4, Table 2).

Consistent with subplot-scale analyses, differences in C_{ha1} vs. C_{ha2} , C_{ha3} , and C_{ha4} were statistically correlated with the quantity of large tree biomass in each hectare of forest, although at this scale, species composition played a clearer role in driving C estimate differences (Fig. 4, Table A3). Specifically, differences between C_{ha1} and C_{ha2} were largest in areas of the forest dominated by angiosperms, suggesting wood CF data for angiosperm species differ most strongly from the wood CF values assumed in these estimates. Alternatively, differences in C_{ha1} vs. C_{ha3} and C_{ha4} values were largest in forests with the highest gymnosperm values (Fig. 4), suggesting the wood CF values assumed in these estimates (i.e., those of the IPCC) differ strongly from actual wood CF values.

At the per ha scale, the 50% wood CF assumption was the only assumption leading to systematic overestimates of C_{ha} values compared to estimates underpinned by species-specific wood CF data (paired t -test $t_9 = -6.6$, $p < 0.01$). Specifically, in comparison to species-specific wood CF data, the 50% assumption overestimated forest C stocks by 2.8 Mg of C ha⁻¹ on average, with overestimates occurring in all 10 hectares of forest analyzed here, ranging from 1.9-3.2 Mg C ha⁻¹ (Fig. 4, Fig. A2). These overestimates were largest in forests dominated by angiosperms, with differences declining with greater gymnosperm biomass (especially large gymnosperms), indicating that the 50% wood CF differs most widely from wood CFs in angiosperms (Fig. 4).

4. Discussion

Studies documenting variability in wood CFs among trees have expanded over the past decade (Doraisami et al., 2022), leading to a considerably greater amount of wood CF data now available for integration with forest C accounting frameworks (Doraisami et al., 2024). Documentation of high variability in wood CFs among co-occurring tree species (e.g., Lamblom and Savidge, 2003; Thomas and Malczewski, 2007) or across forests globally (Martin et al., 2018) implies that this variability systematically influences forest C stocks from individual trees through to global scales. Moreover, much of the literature on wood CF variation makes this case in the context of comparing species-specific wood CF data to a 50% wood CF assumption. Here, studies commonly point to overestimates in C stocks, especially in angiosperm-dominated forests (Martin and Thomas, 2011; Lamblom and Savidge, 2003). To our knowledge, the present study is the first to integrate multiple wood CF assumptions into detailed inventory-based C assessments. In doing so, we find that although certain assertions in the wood CF/forest C accounting literature are supported by our C estimation analysis, there exists considerable nuance surrounding how wood CF variation influences tree- to forest-level C stocks.

Our clearest finding is that a 50% wood CF assumption—historically the value most commonly employed in large-scale studies and national-scale models of forest C stocks and fluxes—consistently overestimates C stocks in comparison to estimates generated using species-specific wood CF data, and that this systematic error compounds across individual trees (C_{tree} ; 0.86 kg of C tree⁻¹ on average), to small spatial scales ($C_{subplot}$; 91.5 kg of C 400 m² on average), and ultimately to larger forest ecosystem scales (C_{ha} ; 2.8 Mg of C ha⁻¹ on average) (Figs. 2-4). Consistent with angiosperms expressing lower wood CFs compared to gymnosperms (Martin et al., 2018), these overestimates are especially prominent in angiosperm trees and angiosperm-dominated forests (Figs. 3, 4).



330 A novel contribution of our study is evidence that while the 50% wood CF assumption systematically
 331 overestimates C across all scales, the size of this error—in absolute C_{tree} , $C_{subplot}$, and C_{ha} terms—is actually smaller
 332 than the error associated with other wood CF assumptions. Our analysis finds that a 50% CF assumption leads to A)
 333 the smallest absolute errors, but simultaneously, B) errors that consistently overestimate C stocks in nearly all trees
 334 and forest stands. To illustrate, a 50% wood CF results in a total estimate of 2,756.2 Mg of C across our 13.5-ha forest
 335 dynamics plot: a value that is 33.7 Mg of C larger than the estimate using species-specific CFs (i.e., 2,722.5 Mg of
 336 C). At larger scales, even if our minimum observed difference between C_{ha1} and C_{ha5} (1.9 Mg C ha^{-1}) is scaled to the
 337 temperate forest biome—estimated at 794,072,373 ha in recent analyses (Pan et al., 2024)—the 50% wood CF
 338 overestimates temperate forest C stocks by 1.5 Pg of C (equivalent to 1,508,737,509 Mg of C). However, if our average
 339 or maximum discrepancy between C_{ha1} and C_{ha5} (2.8 and 3.2 Mg C ha^{-1} , respectively) is scaled in a similar manner,
 340 this overestimate would be equivalent to 2.2–2.5 Pg of C. This value is lower than coarse estimates of similar errors
 341 discussed for tropical forests (Martin and Thomas, 2011), which suggests that the dominance of angiosperms would
 342 lead to differences between our C_{ha1} and C_{ha5} terms that are much larger. Nonetheless, our findings here provide among
 343 the most detailed analyses demonstrating that a 50% wood CF assumption systematically overestimates C stock
 344 estimates at tree, forest ecosystem, and ultimately biome scales.

345 Our analyses of other wood CF assumptions contribute the novel finding that alternative generic CF values—
 346 for example, those recommended by the IPCC (C_{tree4})—generally underestimate C compared to estimates based on
 347 species-specific wood CF data. Here, the influence of wood CF assumptions on C estimation is more nuanced, but
 348 certain trends emerged. First, the magnitude of underestimates depends on tree species identity and DBH at the
 349 individual tree scale (Fig. 2), as well as forest composition and the amount of forest biomass contained in large (≥ 10
 350 cm DBH) trees at the forest scale (Fig. 3, 3). Second, the overall magnitude of these underestimates generally increases
 351 as wood CF assumptions become more generalized from i) temperate biome-specific wood CFs for angiosperms and
 352 gymnosperms (C_{tree2}), to ii) wood CFs for angiosperms and gymnosperms that are not biome-specific (C_{tree3}), and
 353 finally, iii) the IPCC’s default wood CF of 0.47 for all trees (C_{tree4}). We therefore suggest the current IPCC values
 354 recommended for C estimation should be replaced by existing published values, specifically wood CF data for
 355 angiosperms and gymnosperms that are biome-specific (e.g., as presented most recently in (Doraisami et al., 2024)).

356 As expected following previous studies, our analysis found that generalized wood CF assumptions used to
 357 estimate our C_{tree2} – C_{tree5} data approximate the empirically-derived wood CFs (i.e., those used to estimate C_{tree1}) better
 358 for some tree species than others (Fig. 2). This has been well-described by existing studies on wood CF variation
 359 among trees globally (Martin et al., 2018; Thomas and Martin, 2012). Here, we show that the precise wood CF data
 360 are especially important for tree- and forest C stock estimates for large trees (≥ 10 cm DBH) that contribute large
 361 proportions of forest biomass (Fig. 3, Fig. 4). In our study site, large trees represent 87.0–90.0% of total live
 362 aboveground biomass at the 400 m² subplot and per ha scales. In turn, four species, namely balsam fir (*A. balsamea*),
 363 sugar maple (*A. saccharum*), eastern hemlock (*T. canadensis*), and American beech (*F. grandifolia*), represent ~76%
 364 of the large trees in our dataset, with differences in their wood CFs vs. generalized assumptions therefore having a
 365 major influence on C stock estimate discrepancies among methods.



366 Stem wood CFs extracted from open-access databases (Doraisami et al., 2022) and used in our C_{tree1}
 367 calculations for *A. balsamea* and *T. canadensis* were 50.0% and 50.1%, respectively. This likely suggests that forest-
 368 scale overestimates owing to a 50% wood CF assumption (Fig. 4, Fig. A2) may be more constrained in our study site
 369 vs. others where dominant trees differ more widely from a 50% wood CF. Empirically derived wood CFs for these
 370 two gymnosperm species become progressively more different vs. wood CF assumptions embedded in estimates of
 371 C_{tree2} (50.1%), C_{tree3} (48.5%), and C_{tree4} (46.7%). These two species-specific patterns therefore contribute substantially
 372 to our findings that differences in tree- and forest-scale C accounting between $C_{subplot}$ and C_{hal} values vs. all other
 373 estimates (except those based on a 50% assumption) both A) increase with greater wood CF generality and B) are
 374 correlated with large gymnosperm biomass.

375 The most common angiosperms in our datasets, *A. saccharum* and *F. grandifolia*, had empirically derived
 376 wood CF values of 48.4% and 47.9%, respectively (Doraisami et al., 2024). Differences between these species-specific
 377 wood CF values vs. wood CFs embedded in C_{tree2} (46.5%), C_{tree3} (46.8%), and C_{tree4} (46.7%) estimates did not increase
 378 systematically with greater generality of wood CF assumptions. Therefore, except for a 50% wood CF assumption,
 379 C_{tree} values associated with these dominant angiosperms did not necessarily increase or decrease systematically with
 380 more generalized wood CFs (i.e., those used to calculate C_{tree2} , C_{tree3} , and C_{tree4} ; Fig. 2). In turn, our analysis indicates
 381 that while species-specific wood CF data correct for underestimates in angiosperm C stocks compared to all general
 382 wood CF assumptions (except a 50% value), ultimately, discrepancies in C estimates for angiosperm-dominated
 383 forests do not become larger as more general wood CFs are employed in C estimation.

384 One important question raised by our analysis is whether or not the majority of variation in wood CFs exists
 385 among vs. within tree species: a critical question that underpins much of the ecological theory surrounding how plant
 386 diversity influences ecosystem functioning (e.g., Albert et al., 2011; Siefert et al., 2015). If wood CFs vary more
 387 widely among than within tree species, then one might infer that species-specific wood CF values are a “gold standard”
 388 in forest C accounting protocols. This follows logically if, in fact, wood CFs do not vary across factors associated with
 389 intraspecific trait variation, such as environmental conditions or tree age/ size. Meta-analyses have shown that species
 390 identity is the most important factor explaining wood CF differences in the dataset employed in our analysis here,
 391 with intraspecific variation owing to tissue type being less important (Doraisami et al., 2024; Martin et al., 2018).
 392 However, other studies have pointed to variability that exists in wood CFs across tissue types (e.g., Ma et al., 2018),
 393 spatial/ edaphic factors (e.g., Dong et al., 2025), climate gradients (e.g., Paroshy et al., 2021), and tree age/ size (e.g.,
 394 Martin and Thomas, 2013). Nonetheless, these studies aiming to understand how such factors influence wood CFs,
 395 either individually or collectively, are not necessarily definitive. For example, the meta-analysis by Ma et al. (2020)
 396 found that tree DBH or age explained 1-2% of the variability in wood CFs, compared to >85% of the variability
 397 explained by spatial location (a source of intraspecific variability) and species identity (a source of interspecific
 398 variation). We would therefore argue that despite much recent research on the topic, the relative contribution of inter-
 399 vs. intraspecific variability in wood CFs remains only loosely disentangled. Many studies, including our own (Martin
 400 et al., 2013), commonly and in some circumstances unavoidably conflate these different sources of variation. In
 401 relation to our findings here (Figs. 2-4), we suggest that studies isolating the “structure” of intraspecific variation in
 402 wood CFs (sensu Albert et al., 2010) within individual tree species, especially across continuous ranges of tree sizes



403 (e.g., Martin and Thomas, 2013), remains important to better understand how wood chemical trait variation scales up
404 to influence tree and forest C accounting.

405 From an applied perspective, our findings are applicable towards the assessment, monitoring, and potential
406 enhancement of forest C stocks across several management-relevant contexts, frameworks, and scales. At the national
407 scale, our results suggest that the adoption of more species-specific wood CFs into forest C estimation protocols leads
408 to marked changes in C stock estimates, which scale up from the tree-, to forest ecosystem-, and ultimately to biome
409 scales. Our findings suggest that species-specific wood CFs should be employed when estimating forest C stocks and
410 fluxes, though when not available, alternative wood CFs other than a 50% wood CF are likely to provide a more
411 conservative estimate of forest C stocks and fluxes. Additionally, and consistent with research on the critical role that
412 large trees play in forest ecosystem functioning (e.g., Lutz et al., 2018), our results suggest that careful consideration
413 of wood CFs among common trees that contribute the most to large stem biomass is especially important in accurately
414 accounting for C stocks and fluxes in trees and forests.

415



Table 1. Summary statistics of carbon stock estimates at tree⁻¹ (kg of C), 400 m⁻² subplot (kg of C), and ha⁻¹ (Mg of C) scales, generated using five different wood carbon fraction (CF) assumptions. Descriptive statistics presented here are based on $n=39,064$ trees (for C_{tree}), $n=368$ subplots (for $C_{subplot}$), and $n=10$ ha (for C_{ha}).

Carbon estimators and wood CF assumptions			Central tendency			Range		Distributions				
Scale	Estimate	Description of estimate	Mean	Median	S.D.	Min.	Max.	0.05	0.1	0.9	0.95	IQR
Tree-level (kg C tree ⁻¹)	C_{tree1}	Species-specific wood CF	69.695	2.353	263.206	0.045	7,783.824	0.113	0.173	167.685	370.583	16.654
	C_{tree2}	Division- and biome wood CF	68.889	2.283	262.654	0.043	7,799.391	0.110	0.170	163.370	363.311	16.515
	C_{tree3}	Division-specific wood CF	67.586	2.298	255.325	0.044	7,550.309	0.111	0.169	162.654	359.401	16.131
	C_{tree4}	IPCC C conversion factor	65.900	2.267	246.859	0.044	7,270.091	0.111	0.168	160.081	352.593	15.845
	C_{tree5}	50% C conversion factor	70.557	2.428	264.303	0.047	7,783.824	0.119	0.180	171.393	377.508	16.965
Subplot (kg C 400m ⁻²)	$C_{subplot1}$	Species-specific wood CF	7,398.1	4,443.00	7,620.25	10.36	45,387.39	1,318.61	2,350.09	16,886.63	22,791.41	5,470.102
	$C_{subplot2}$	Division- and biome wood CF	7,312.6	4,313.36	7,640.96	9.47	45,397.22	1,303.79	2,269.55	16,857.13	22,705.73	5,520.831
	$C_{subplot3}$	Division-specific wood CF	7,174.3	4,319.16	7,392.15	9.50	44,023.68	1,269.56	2,272.43	16,377.18	22,103.26	5,308.894
	$C_{subplot4}$	IPCC C conversion factor	6,995.3	4,278.03	7,113.72	9.45	42,459.75	1,254.71	2,245.66	15,869.13	21,395.42	5,053.282
	$C_{subplot5}$	50% C conversion factor	7,489.6	4,580.33	7,616.40	10.12	45,460.12	1,343.37	2,404.35	16,990.50	22,907.31	5,410.367
Hectare (Mg C ha ⁻¹)	C_{ha1}	Species-specific wood CF	175.7	137.4	110.4	83.3	383.8	87.3	91.3	375.8	379.8	48.6
	C_{ha2}	Division- and biome wood CF	173.1	134.4	111.1	80.1	382.5	84.2	88.2	374.4	378.5	48.4
	C_{ha3}	Division-specific wood CF	170.5	133.2	107.1	80.6	372.3	84.6	88.6	364.5	368.4	47.1
	C_{ha4}	IPCC C conversion factor	166.8	131.2	102.5	80.5	360.4	84.4	88.2	352.8	356.6	45.5
	C_{ha5}	50% C conversion factor	178.5	140.4	110.0	86.1	385.8	90.3	94.5	377.7	381.8	48.7

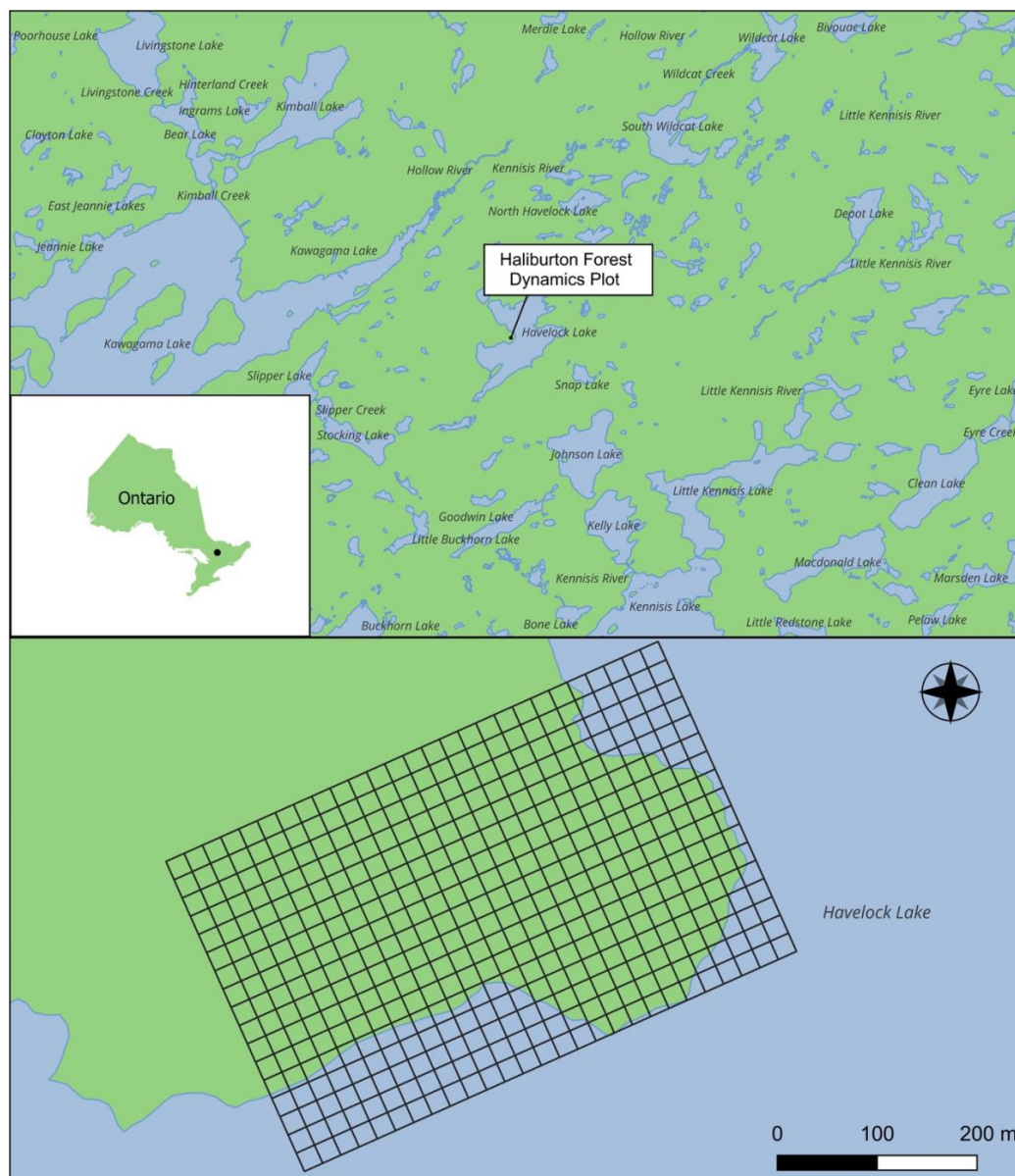


Table 2. Summary statistics of carbon stock differences calculated at tree⁻¹ (kg of C), 400 m⁻² subplot (kg of C), and ha⁻¹ (Mg of C) scales, generated using five different wood carbon fraction (CF) assumptions. In these calculations, C estimates at all scales are generated by converting tree-level biomass to C with species-specific wood CF data (C_{tree1} , C_{subplot1} , and C_{ha1} , as described in Table 1). Therefore, positive differences denote instances where more generalized wood CF assumptions underestimate tree-, subplot-, and per ha C stock estimates (i.e., $C_{\text{tree2}}-C_{\text{tree4}}$, $C_{\text{subplot2}}-C_{\text{subplot4}}$, $C_{\text{ha2}}-C_{\text{ha4}}$), while negative values denote instances where generalized wood CF assumptions overestimate tree-, subplot-, and per ha C stock estimates (i.e., C_{tree5} , C_{subplot5} , C_{ha5}). Also shown are paired *t*-tests evaluating statistical differences in all estimate comparisons, where $n=39,064$ trees (C_{tree}), $n=368$ subplots (C_{subplot}), and $n=10$ ha (C_{ha}). Summary statistics and raw values are presented visually in Fig. 2 (for C_{tree} comparisons), Fig. 3 (for C_{subplot} comparisons), and Fig. 4 (for C_{ha} comparisons).

Scale	Carbon estimate comparison	Mean difference	Min. difference	Max. difference	<i>t</i> -value (<i>p</i> -value)
Tree-level (kg C tree ⁻¹)	$C_{\text{tree1}} - C_{\text{tree2}}$	0.803	-15.568	83.627	$t_{39,063}=255.9$ ($p<0.01$)
	$C_{\text{tree1}} - C_{\text{tree3}}$	2.109	-0.149	233.515	$t_{39,063}=526.0$ ($p<0.01$)
	$C_{\text{tree1}} - C_{\text{tree4}}$	3.795	-0.099	513.732	$t_{39,063}=385.3$ ($p<0.01$)
	$C_{\text{tree1}} - C_{\text{tree5}}$	-0.862	-88.328	11.482	$t_{39,063}=-263.8$ ($p<0.01$)
Subplot (kg C 400m ⁻²)	$C_{\text{subplot1}} - C_{\text{subplot2}}$	85.5	-29.7	225.9	$t_{367}=25.2$ ($p<0.01$)
	$C_{\text{subplot1}} - C_{\text{subplot3}}$	223.9	0.6	1363.7	$t_{367}=92.8$ ($p<0.01$)
	$C_{\text{subplot1}} - C_{\text{subplot4}}$	402.9	0.9	2,927.7	$t_{367}=62.0$ ($p<0.01$)
	$C_{\text{subplot1}} - C_{\text{subplot5}}$	-91.5	-267.3	16.4	$t_{367}=-24.1$ ($p<0.01$)
Hectare (Mg C ha ⁻¹)	$C_{\text{ha1}} - C_{\text{ha2}}$	2.6	1.3	3.3	$t_9=5.8$ ($p<0.01$)
	$C_{\text{ha1}} - C_{\text{ha3}}$	5.3	2.6	11.5	$t_9=108.1$ ($p<0.01$)
	$C_{\text{ha1}} - C_{\text{ha4}}$	9.0	2.8	23.5	$t_9=15.0$ ($p<0.01$)
	$C_{\text{ha1}} - C_{\text{ha5}}$	-2.8	-3.2	-1.9	$t_9=-6.7$ ($p<0.01$)



433



434

435 **Fig. 1.** Geographical location of the Haliburton Forest Dynamics Plot (HFDP) situated in Haliburton County, Ontario,
 436 Canada. Panels A and B represent the location of the HFDP within provincial and regional contexts, respectively, while
 437 Panel C represents the extent of the 13.5-ha HFDP as subdivided into $n=368$ subplots of 400 m² (20-by-20 m) in size.
 438

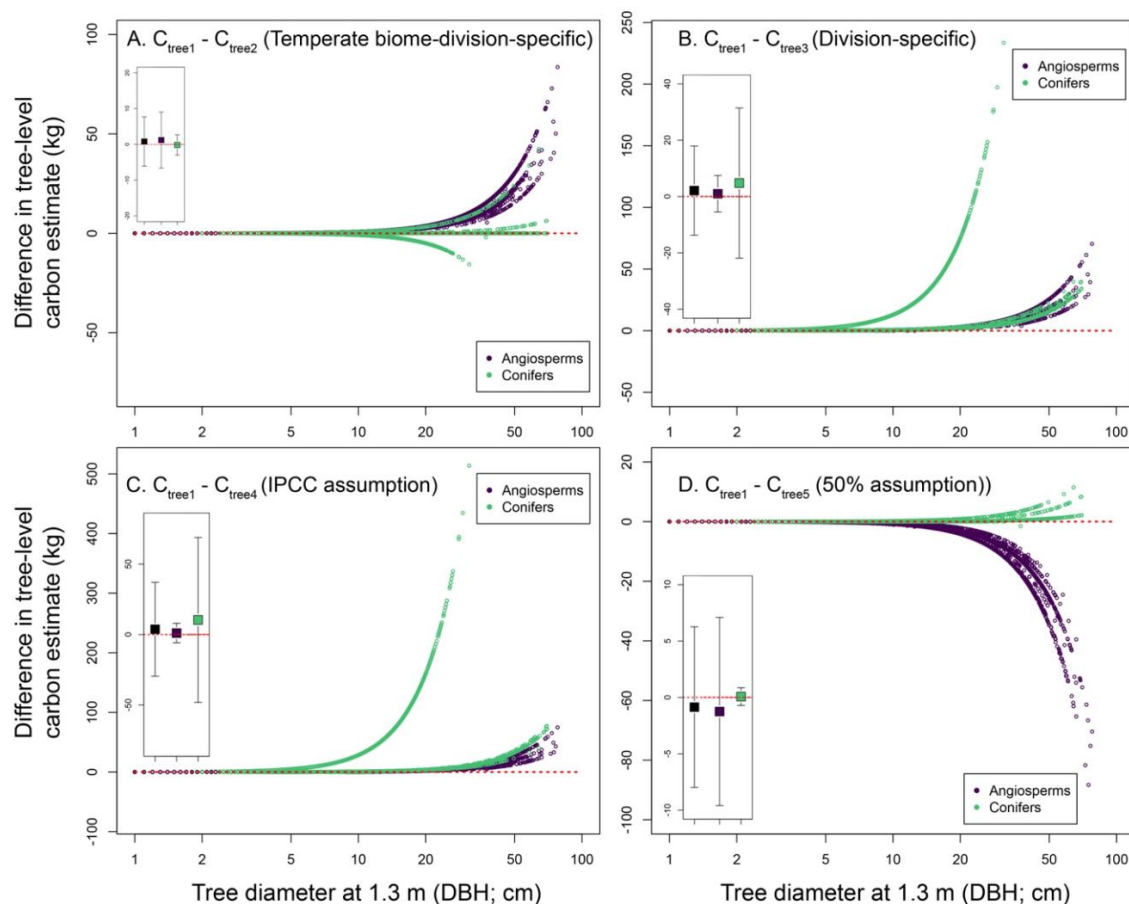
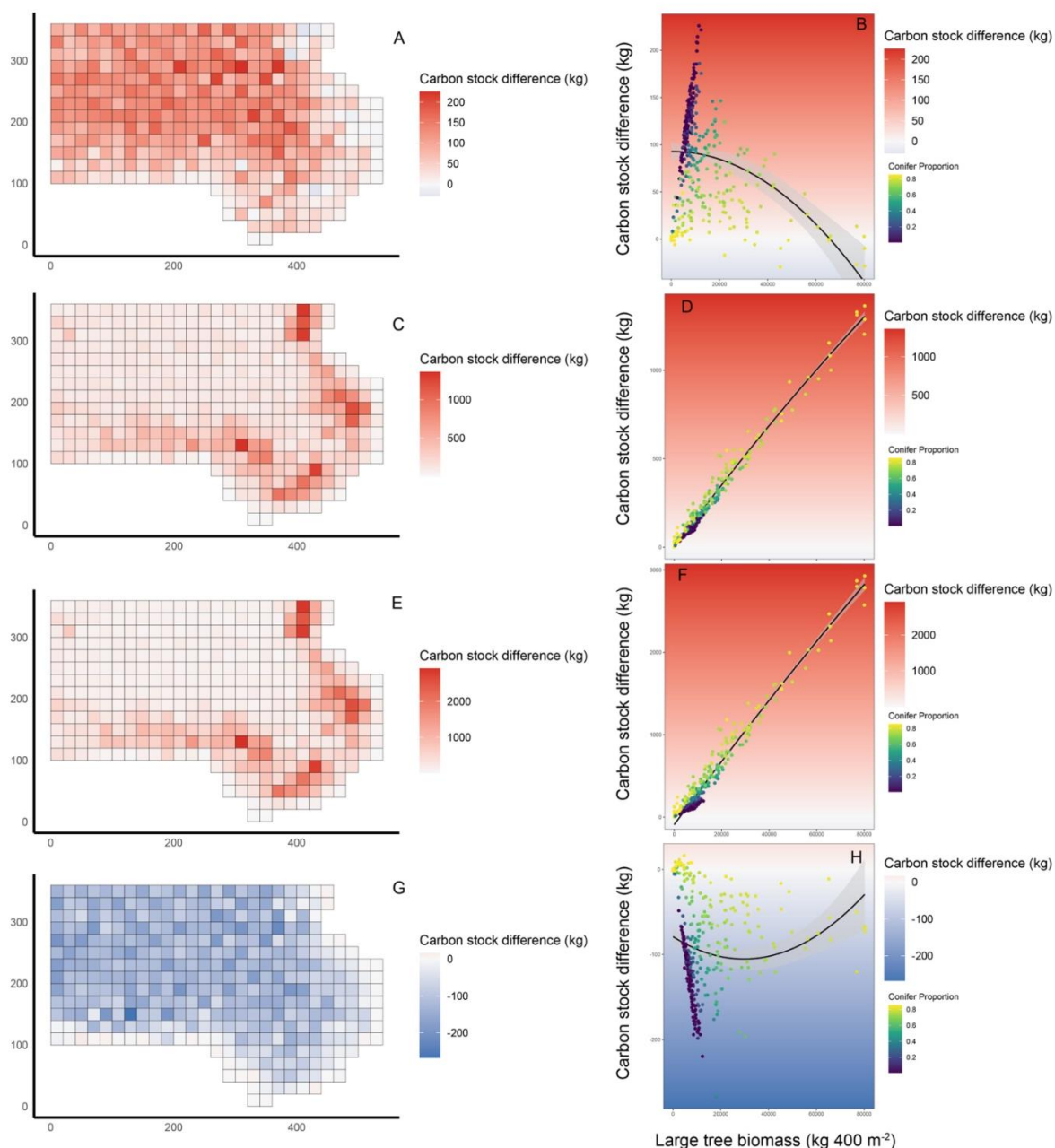


Fig. 2. Differences in tree-level carbon (C) stocks (measured in kg C tree⁻¹) estimated using different wood carbon fraction (CF) assumptions. Main panels show differences in tree-level C stocks for $n=39,064$ trees distributed across angiosperms ($n=27,589$; purple open points) and gymnosperms ($n=11,475$; green open points), calculated as the difference between C_{tree1} (generated using species-specific wood CF data) and C_{tree2} (Panel A; generated assuming wood CFs for temperate biome trees specific to gymnosperms and angiosperms); C_{tree3} (Panel B; generated assuming non-biome-specific wood CFs for gymnosperms and angiosperms); C_{tree4} (Panel C; generated assuming a single IPCC default wood CF assumption); and C_{tree5} (Panel D; generated assuming a single 50% wood CF assumption). Red dotted lines denote 0 differences in tree-level C stock estimates, such that i) all values above 0 indicate instances where species-specific wood CFs (C_{tree1}) are higher compared to estimates generated using generalized wood CF assumptions ($C_{tree2}-C_{tree5}$), and ii) all values below 0 indicate instances where species-specific wood CFs (C_{tree1}) are lower compared to estimates generated using generalized wood CF assumptions ($C_{tree2}-C_{tree5}$). Inset graphs in each panel represent mean differences in C_{tree} estimates (calculated as in the main panels) across all



453 trees (black symbols), angiosperms (purple filled symbols), and gymnosperms (green filled symbols), with error bars
454 denoting 2 standard deviations about the mean.



455
 456 **Fig. 3.** Differences in 400-m² subplot-level carbon (C_{subplot}) stocks (measured in kg C subplot⁻¹) estimated using
 457 different wood carbon fraction (CF) assumptions. Subplot-level differences are calculated as the difference between
 458 C_{subplot1} (generated using species-specific wood CF data) and C_{subplot2} (Panels A-B; generated assuming wood CFs for



temperate biome trees specific to gymnosperms and angiosperms); C_{subplot3} (Panels C-D; generated assuming non-
 biome-specific wood CFs for gymnosperms and angiosperms); C_{subplot4} (Panels E-F; generated assuming a single
 IPCC default wood CF assumption); and C_{subplot5} (Panel G-H; generated assuming a single 50% wood CF
 assumption). Therefore in all maps and graphs, i) all values above 0 and in red shading indicate instances where
 species-specific wood CFs (C_{subplot1}) are higher compared to estimates generated using generalized wood CF
 assumptions ($C_{\text{subplot2}}-C_{\text{subplot5}}$), and ii) all values below 0 and in blue shading indicate instances where species-
 specific wood CFs (C_{subplot1}) are lower compared to estimates generated using generalized wood CF assumptions
 ($C_{\text{subplot2}}-C_{\text{subplot5}}$). Left-side panels show spatial variability in differences between subplot-level C stocks for $n=368$
 subplots distributed across a 13.5-ha forest dynamics plot in Haliburton, Ontario, Canada. Right-hand panels shows
 statistically significant relationships between differences in C stock estimates (as described above) modeled as a
 function of large tree biomass (≥ 10 cm diameter at 1.3 m aboveground) in each subplot, and a second-order
 polynomial term for large tree biomass. Error bars represent 95% confidence limits surrounding model fits, and
 point colors correspond to the proportion of biomass represented by gymnosperms in each subplot (a full analysis of
 covariance model parameters for each fit is presented in Table A2).

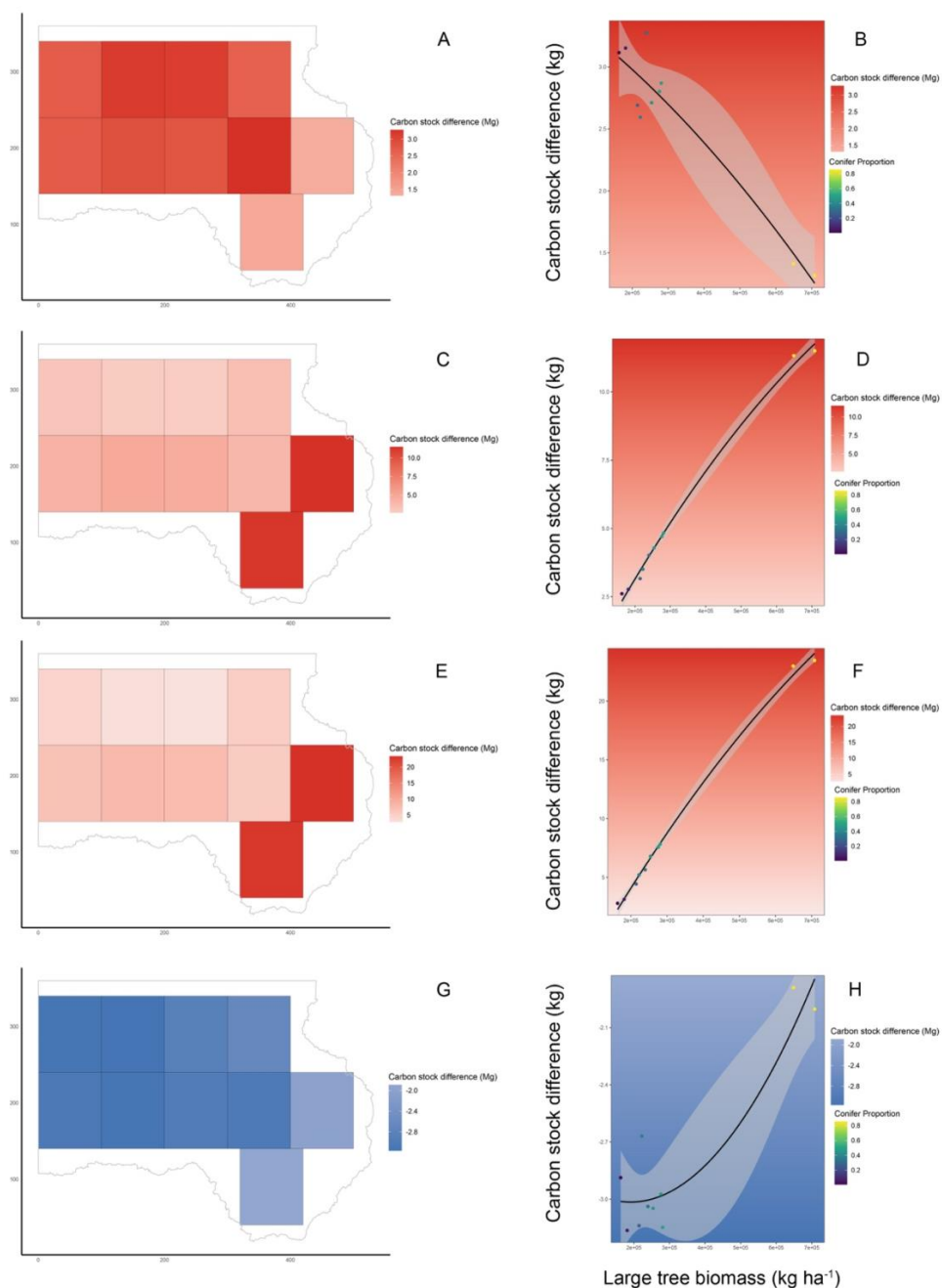


Fig. 4. Differences in ha-scale carbon (C_{ha}) stocks (measured in $Mg\ C\ ha^{-1}$) estimated using different wood carbon fraction (CF) assumptions. Per ha-level differences are calculated as the difference between C_{ha1} (generated using



476 species-specific wood CF data) and C_{ha2} (Panels A-B; generated assuming wood CFs for temperate biome trees
 477 specific to gymnosperms and angiosperms); C_{ha3} (Panels C-D; generated assuming non-biome-specific wood CFs
 478 for gymnosperms and angiosperms); C_{ha4} (Panels E-F; generated assuming a single IPCC default wood CF
 479 assumption); and C_{ha5} (Panel G-H; generated assuming a single 50% wood CF assumption). Therefore in all maps
 480 and graphs, i) all values above 0 and in red shading indicate instances where species-specific wood CFs (C_{ha1}) are
 481 higher compared to estimates generated using generalized wood CF assumptions (C_{ha2} - C_{ha5}), and ii) all values below
 482 0 and in blue shading indicate instances where species-specific wood CFs (C_{ha1}) are lower compared to estimates
 483 generated using generalized wood CF assumptions (C_{ha2} - C_{ha5}). Left-side panels show spatial variability in
 484 differences in subplot-level C stocks for $n=10$ ha designations distributed across a 13.5-ha forest dynamics plot in
 485 Haliburton, Ontario, Canada. Right-hand panels shows statistically significant relationships between differences in C
 486 stock estimates (as described above) modeled as a function of large tree biomass (≥ 10 cm diameter at 1.3 m
 487 aboveground) in each ha of forest, and a second-order polynomial term for large tree biomass. In these graphs, error
 488 bars represent 95% confidence limits surrounding model fits, and point colors correspond to the proportion of
 489 biomass represented by gymnosperms in each ha of forest (a full analysis of covariance model parameters for each
 490 fit is presented in Table A3).



491 **Code availability**

492 No custom code were used in the analysis presented here, though code is available upon request to the corresponding
 493 author.

494
 495 **Availability of data**

496 Data for this research are available through the Forest Global Earth Observatory Network data portal.

497
 498 **Author contributions**

499 Data collection: A.R.M., M.D., M.G., R.M., L.S., S.C.T.

500 Data analysis: A.R.M., D.M., M.D.

501 Manuscript writing: A.R.M., D.M.

502 Manuscript editing: M.D., M.G., A.G., D.O., A.B.P., B.T., R.O.M., L.S., S.C.T.

503 Funding acquisition and logistics: A.R.M., A.G., D.O., A.B.P., B.T., S.C.T.

504
 505 **Competing interests**

506 The authors declare no competing interests.

507
 508 **Acknowledgements**

509 The authors wish to thank the numerous field researchers who assisted in the collection of field data from the
 510 Haliburton Forest Dynamics Plot, as well as the Haliburton Forest & Wild Life Reserve for continued support of the
 511 Haliburton Forest Dynamics Plot and the Forest Global Earth Observatory program.

512
 513 **Financial support**

514 This research was supported by the Charles Bullard Fellowship in Forest Research to A.R.M. Funding for the
 515 Haliburton Forest Dynamics Plot was supported by Discovery Grants from the Natural Sciences and Engineering
 516 Research Council of Canada to both A.R.M. and S.C.T.

517
 518 **References**

- 519 Albert, C. H., Grassein, F., Schurr, F. M., Vieilledent, G., and Violle, C.: When and how should intraspecific
 520 variability be considered in trait-based plant ecology?, *Perspectives in Plant Ecology, Evolution and Systematics*, 13,
 521 217-225, 2011.
- 522 Albert, C. H., Thuiller, W., Yoccoz, N. G., Soudant, A., Boucher, F., Saccone, P., and Lavorel, S.: Intraspecific
 523 functional variability: extent, structure and sources of variation, *Journal of Ecology*, 98, 604-613, 2010.
- 524 Anderegg, W. R., Hicke, J. A., Fisher, R. A., Allen, C. D., Aukema, J., Bentz, B., Hood, S., Lichstein, J. W., Macalady,
 525 A. K., and McDowell, N.: Tree mortality from drought, insects, and their interactions in a changing climate, *New*
 526 *Phytologist*, 208, 674-683, 2015.



- 527 Coops, N. C., Tompalski, P., Goodbody, T. R., Queinnec, M., Luther, J. E., Bolton, D. K., White, J. C., Wulder, M.
- 528 A., van Lier, O. R., and Hermosilla, T.: Modelling lidar-derived estimates of forest attributes over space and time: a
- 529 review of approaches and future trends, *Remote Sensing of Environment*, 260, 112477, 2021.
- 530 Davies, S. J., Abiem, I., Salim, K. A., Aguilar, S., Allen, D., Alonso, A., Anderson-Teixeira, K., Andrade, A., Arellano,
- 531 G., and Ashton, P. S.: ForestGEO: Understanding forest diversity and dynamics through a global observatory network,
- 532 *Biological Conservation*, 253, 108907, 2021.
- 533 Domke, G. M., Oswalt, S. N., Walters, B. F., and Morin, R. S.: Tree planting has the potential to increase carbon
- 534 sequestration capacity of forests in the United States, *Proceedings of the National Academy of Sciences*, 117, 24649-
- 535 24651, 2020.
- 536 Dong, C., Liu, Y., Zhang, L., Liu, Z., Zhao, H., Li, W., Chao, X., and Wang, X.: Spatial Patterns of Stem Tissue
- 537 Carbon Content in Fagaceae Species from Typical Forests in China, *Forests*, 16, 1478, 2025.
- 538 Doraisami, M., Domke, G. M., and Martin, A. R.: Improving wood carbon fractions for multiscale forest carbon
- 539 estimation, *Carbon Balance and Management*, 19, 25, 2024.
- 540 Doraisami, M., Kish, R., Paroshy, N. J., Domke, G. M., Thomas, S. C., and Martin, A. R.: A global database of woody
- 541 tissue carbon concentrations, *Scientific Data*, 9, 284, 2022.
- 542 Harris, N. L., Gibbs, D. A., Baccini, A., Birdsey, R. A., De Bruin, S., Farina, M., Fatoyinbo, L., Hansen, M. C., Herold,
- 543 M., and Houghton, R. A.: Global maps of twenty-first century forest carbon fluxes, *Nature Climate Change*, 11, 234-
- 544 240, 2021.
- 545 Hartmann, H., Bastos, A., Das, A. J., Esquivel-Muelbert, A., Hammond, W. M., Martínez-Vilalta, J., McDowell, N.
- 546 G., Powers, J. S., Pugh, T. A., and Ruthrof, K. X.: Climate change risks to global forest health: emergence of
- 547 unexpected events of elevated tree mortality worldwide, *Annual Review of Plant Biology*, 73, 673-702, 2022.
- 548 Hogan, J. A., Domke, G. M., Zhu, K., Johnson, D. J., and Lichstein, J. W.: Climate change determines the sign of
- 549 productivity trends in US forests, *Proceedings of the National Academy of Sciences*, 121, e2311132121, 2024.
- 550 IPCC: IPCC guidelines for national greenhouse gas inventories, prepared
- 551 by the national greenhouse gas inventories programme, 2006.
- 552 Kish, R., James, P. M., Mariani, R. O., Schurman, J. S., Thomas, S. C., Young, E. N., and Martin, A. R.: Beech Bark
- 553 Disease in an unmanaged temperate forest: patterns, predictors, and impacts on ecosystem function, *Frontiers in*
- 554 *Forests and Global Change*, 5, 831663, 2022.
- 555 Lambert, M.-C., Ung, C., and Raulier, F.: Canadian national tree aboveground biomass equations, *Canadian Journal*
- 556 *of Forest Research*, 35, 1996-2018, 2005.
- 557 Lamtom, S. and Savidge, R.: A reassessment of carbon content in wood: variation within and between 41 North
- 558 American species, *Biomass and Bioenergy*, 25, 381-388, 2003.
- 559 Lutz, J. A., Furniss, T. J., Johnson, D. J., Davies, S. J., Allen, D., Alonso, A., Anderson-Teixeira, K. J., Andrade, A.,
- 560 Baltzer, J., and Becker, K. M.: Global importance of large-diameter trees, *Global Ecology and Biogeography*, 27, 849-
- 561 864, 2018.
- 562 Ma, S., He, F., Tian, D., Zou, D., Yan, Z., Yang, Y., Zhou, T., Huang, K., Shen, H., and Fang, J.: Variations and
- 563 determinants of carbon content in plants: a global synthesis, *Biogeosciences*, 15, 693-702, 2018.



564 Ma, S.-H., Eziz, A., Tian, D., Yan, Z.-B., Cai, Q., Jiang, M.-W., Ji, C.-J., and Fang, J.-Y.: Size-and age-dependent
 565 increases in tree stem carbon concentration: implications for forest carbon stock estimations, *Journal of Plant Ecology*,
 566 13, 233-240, 2020.

567 Martin, A. R. and Thomas, S. C.: A reassessment of carbon content in tropical trees, *PloS ONE*, 6, e23533, 2011.

568 Martin, A. R. and Thomas, S. C.: Size-dependent changes in leaf and wood chemical traits in two Caribbean rainforest
 569 trees, *Tree physiology*, 33, 1338-1353, 2013.

570 Martin, A. R., Doraisami, M., and Thomas, S. C.: Global patterns in wood carbon concentration across the world's
 571 trees and forests, *Nature Geoscience*, 11, 915-920, 2018.

572 Martin, A. R., Gezahegn, S., and Thomas, S. C.: Variation in carbon and nitrogen concentration among major woody
 573 tissue types in temperate trees, *Canadian Journal of Forest Research*, 45, 744-757, 2015.

574 Martin, A. R., Thomas, S. C., and Zhao, Y.: Size-dependent changes in wood chemical traits: a comparison of
 575 neotropical saplings and large trees, *AoB Plants*, 5, plt039, 2013.

576 Pan, Y., Birdsey, R. A., Phillips, O. L., Houghton, R. A., Fang, J., Kauppi, P. E., Keith, H., Kurz, W. A., Ito, A., and
 577 Lewis, S. L.: The enduring world forest carbon sink, *Nature*, 631, 563-569, 2024.

578 Paroshy, N. J., Doraisami, M., Kish, R., and Martin, A. R.: Carbon concentration in the world's trees across climatic
 579 gradients, *New Phytologist*, 232, 123-133, 2021.

580 Siefert, A., Violle, C., Chalmandrier, L., Albert, C. H., Taudiere, A., Fajardo, A., Aarssen, L. W., Baraloto, C.,
 581 Carlucci, M. B., and Cianciaruso, M. V.: A global meta-analysis of the relative extent of intraspecific trait variation
 582 in plant communities, *Ecology letters*, 18, 1406-1419, 2015.

583 Simler-Williamson, A. B., Rizzo, D. M., and Cobb, R. C.: Interacting effects of global change on forest pest and
 584 pathogen dynamics, *Annual Review of Ecology, Evolution, and Systematics*, 50, 381-403, 2019.

585 Thomas, S. and Malczewski, G.: Wood carbon content of tree species in Eastern China: Interspecific variability and
 586 the importance of the volatile fraction, *Journal of Environmental Management*, 85, 659-662, 2007.

587 Thomas, S. C. and Martin, A. R.: Carbon content of tree tissues: a synthesis, *Forests*, 3, 332-352, 2012.

588 Weed, A. S., Ayres, M. P., and Hicke, J. A.: Consequences of climate change for biotic disturbances in North American
 589 forests, *Ecological Monographs*, 83, 441-470, 2013.

590 Xu, L., Saatchi, S. S., Yang, Y., Yu, Y., Pongratz, J., Bloom, A. A., Bowman, K., Worden, J., Liu, J., and Yin, Y.:
 591 Changes in global terrestrial live biomass over the 21st century, *Science Advances*, 7, eabe9829, 2021.

592 Yang, H., Ciais, P., Frappart, F., Li, X., Brandt, M., Fensholt, R., Fan, L., Saatchi, S., Besnard, S., and Deng, Z.:
 593 Global increase in biomass carbon stock dominated by growth of northern young forests over past decade, *Nature*
 594 *Geoscience*, 16, 886-892, 2023.

595



596 Appendices

597

598 Appendix A

599

600 **Table A1.** Parameters from an Analysis of covariance (ANCOVA) model predicting differences in tree-level carbon
 601 (C) estimates (measured in kg C tree⁻¹) as a function of an intercept term (corresponding to an average C stock
 602 difference among C_{tree} estimates), taxonomic division (as a categorical factor), DBH, a second-order polynomial
 603 DBH term (DBH²), as well as division-by-DBH and division-by-DBH² interaction terms. Differences in tree-level C
 604 estimates were calculated based on five separate tree-level C estimates, denoted as C_{tree} as follows: C_{tree1}) generated
 605 using species-specific wood CF data; C_{tree2}) generated assuming wood CFs for temperate biome trees specific to
 606 conifers and angiosperms; C_{tree3}) generated assuming non-biome-specific wood CFs for conifers and angiosperms;
 607 C_{tree4}) generated assuming a single IPCC default wood CF assumption; C_{tree5}) generated assuming a single 50%
 608 wood CF assumption. The taxonomic division term is based on a categorical variable with two values (angiosperm
 609 and conifer), such that angiosperms are the reference group in ANCOVA models. Sample sizes for all four
 610 ANCOVA models was $n=39,064$ trees distributed across angiosperms ($n=27,589$) and conifers ($n=11,475$).

C estimation difference	Parameter	Estimate	Std. Error	<i>t</i> (<i>p</i> -value)	Partial <i>r</i> ²	Model <i>p</i>	Model <i>r</i> ²
C _{tree1} - C _{tree2}	Intercept	0.101	0.01	10.4 (<0.001)	0.003	<0.001	0.9151
	Conifer	0.127	0.02	6.3 (<0.001)	0.001		
	DBH	-0.063	0.002	-34.3 (<0.001)	0.029		
	DBH ²	0.011	0.00004	257.5 (<0.001)	0.629		
	Conifer * DBH	-0.026	0.003	-8.2 (<0.001)	0.002		
	Conifer * DBH ²	-0.009	0.0001	-119.6 (<0.001)	0.268		
C _{tree1} - C _{tree3}	Intercept	0.064	0.063	1.0 (0.311)	0.000	<0.001	0.3257
	Conifer	-3.947	0.13	-30.3 (<0.001)	0.023		
	DBH	-0.046	0.012	-3.9 (<0.001)	0.000		
	DBH ²	0.009	0.0003	32.2 (<0.001)	0.026		
	Conifer * DBH	1.385	0.021	66.0 (<0.001)	0.100		
	Conifer * DBH ²	-0.028	0.001	-57.2 (<0.001)	0.077		
C _{tree1} - C _{tree4}	Intercept	0.076	0.138	0.6 (0.583)	0.000	<0.001	0.2656
	Conifer	-8.591	0.287	-30.0 (<0.001)	0.022		
	DBH	-0.051	0.026	-2.0 (0.048)	0.000		
	DBH ²	0.01	0.001	15.8 (<0.001)	0.006		
	Conifer * DBH	3.0	0.046	65.0 (<0.001)	0.097		
	Conifer * DBH ²	-0.052	0.001	-48.7 (<0.001)	0.057		
C _{tree1} - C _{tree5}	Intercept	-0.33	0.006	-56.5 (<0.001)	0.076	<0.001	0.9714
	Conifer	0.36	0.012	29.6 (<0.001)	0.022		



	DBH	0.133	0.001	120.7 (<0.001)	0.272		
	DBH ²	-0.014	0.00003	-513.3 (<0.001)	0.871		
	Conifer * DBH	-0.143	0.002	-73.6 (<0.001)	0.122		
	Conifer * DBH ²	0.015	0.00004	325.1 (<0.001)	0.730		

611



Table A2. Parameters from linear models predicting differences in 400-m² subplot-level carbon (C) estimates (measured in kg C subplot⁻¹) as a function of an intercept term (corresponding to an average C stock difference among C_{subplot} estimates), as well as the following subplot-scale variables: large tree (i.e., ≥10 cm DBH) biomass, small tree (1-10 cm DBH) biomass, second-order polynomial terms of large and small tree, and the proportion of total biomass represented by conifer tree species. Differences in subplot-level C estimates were calculated based on five separate tree-level C estimates, denoted as C_{tree} as follows: C_{subplot1}) generated using species-specific wood CF data; C_{subplot2}) generated assuming wood CFs for temperate biome trees specific to conifers and angiosperms; C_{subplot3}) generated assuming non-biome-specific wood CFs for conifers and angiosperms; C_{subplot4}) generated assuming a single IPCC default wood CF assumption; C_{subplot5}) generated assuming a single 50% wood CF assumption. Sample sizes for all four linear models was $n=368$ 400-m² subplots (presented visually in Fig. 3).

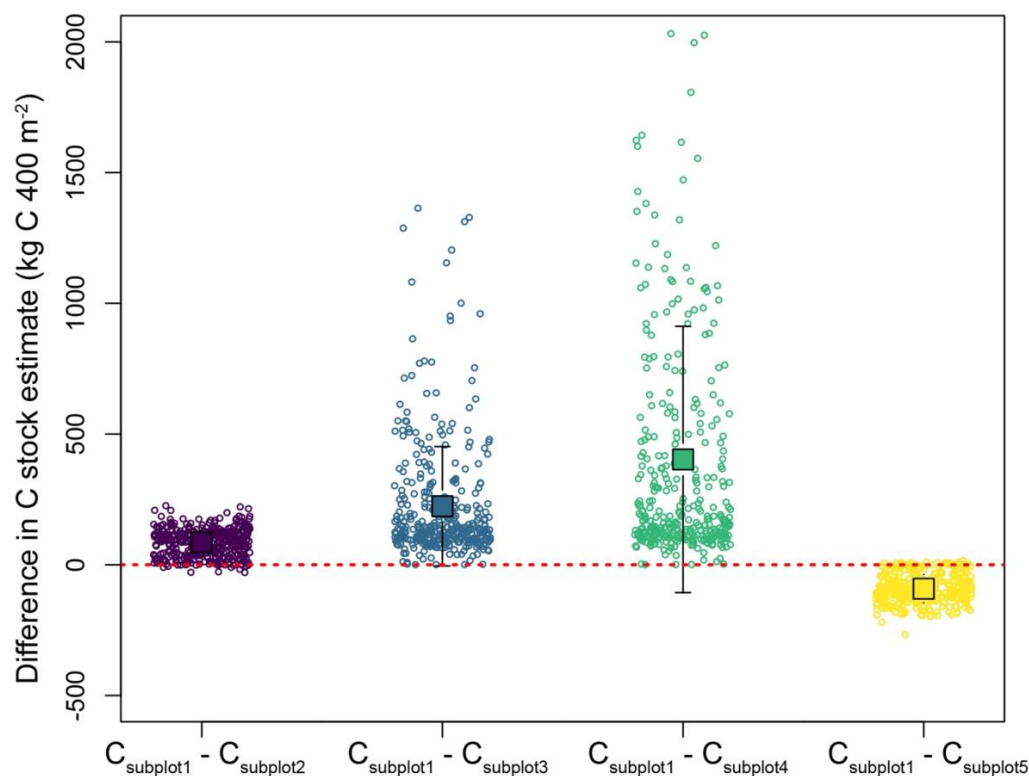
C estimation difference	Parameter	Estimate	Std. Error	t (p-value)	Partial r ²	Model r ²	Model p
C _{subplot1} - C _{subplot2}	Intercept	111.3	2.859	39.0 (<0.01)	0.81	0.7648	<0.001
	Large tree biomass	0.004	0.0004	10.5 (<0.01)	0.221		
	Large tree biomass ²	0.0001	0.0001	-10.4 (<0.01)	0.235		
	Small tree biomass	0.001	0.002	0.3 (0.776)	0.0002		
	Small tree biomass ²	0.0001	0.0001	-1.2 (0.237)	0.004		
	Conifer proportion	-120.4	4.652	-25.9 (<0.01)	0.654		
C _{subplot1} - C _{subplot3}	Intercept	0.37	1.246	0.295 (0.769)	0.0002		
	Large tree biomass	0.0143	0.0002	93.0 (<0.01)	0.961	0.9975	<0.001
	Large tree biomass ²	0.0001	0.0001	3.2 (0.002)	0.027		
	Small tree biomass	0.02	0.002	18.3 (<0.01)	0.487		
	Small tree biomass ²	0.0001	0.0001	1.1 (0.258)	0.004		
	Conifer proportion	11.85	2.03	5.8 (<0.01)	0.088		
C _{subplot1} - C _{subplot4}	Intercept	-98.91	3.22	-30.8 (<0.01)	0.727		
	Large tree biomass	0.03	0.001	69.6 (<0.01)	0.932	0.9967	<0.001
	Large tree biomass ²	0.0001	0.0001	10.6 (<0.01)	0.241		
	Small tree biomass	0.03	0.002	15.0 (<0.01)	0.389		
	Small tree biomass ²	0.0001	0.0001	1.8 (<0.01)	0.009		
	Conifer proportion	130.2	5.24	24.9 (<0.01)	0.635		
C _{subplot1} - C _{subplot5}	Intercept	-98.91	3.22	-30.8 (<0.01)	0.727		
	Large tree biomass	-0.01	0.001	-13.4 (<0.01)	0.335	0.7166	<0.001
	Large tree biomass ²	0.0001	0.0001	10.6 (<0.01)	0.241		
	Small tree biomass	-0.002	0.002	-1.1 (0.292)	0.003		
	Small tree biomass ²	0.0001	0.0001	1.8 (0.077)	0.009		
	Conifer proportion	130.2	5.24	24.9 (<0.01)	0.635		

622



Table A3. Parameters from linear models predicting differences in per ha carbon (C) estimates (measured in Mg C subplot⁻¹) predicted as a function of an intercept term (corresponding to an average C stock difference), as well as the following per ha-scale variables: large tree (i.e., ≥ 10 cm DBH) biomass, small tree (1-10 cm DBH) biomass, second-order polynomial terms of large and small tree, and the proportion of total biomass represented by conifer tree species. Differences in per ha C estimates were calculated based on five separate tree-level C estimates, denoted as C_{tree} as follows: C_{ha1}) generated using species-specific wood CF data; C_{ha2}) generated assuming wood CFs for temperate biome trees specific to conifers and angiosperms; C_{ha3}) generated assuming non-biome-specific wood CFs for conifers and angiosperms; C_{ha4}) generated assuming a single IPCC default wood CF assumption; C_{ha5}) generated assuming a single 50% wood CF assumption. Sample sizes for all four linear models was $n=10$ has (presented visually in Fig. 4).

C estimation difference	Parameter	Estimate	Std. Error	t (p -value)	Partial r^2	Model r^2	Model p
$C_{\text{ha1}} - C_{\text{ha2}}$	Intercept	-1487.0	1440.0	-1.0 (0.36)	0.211	0.966	<0.001
	Large tree biomass	0.033	0.01	3.2 (0.034)	0.716		
	Large tree biomass ²	0.0001	0.0001	-3.4 (0.028)	0.741		
	Small tree biomass	0.007	0.01	0.7 (0.538)	0.102		
	Small tree biomass ²	0.0001	0.0001	-2.0 (0.112)	0.509		
	Conifer proportion	-4998.0	1157.0	-4.3 (0.012)	0.824		
$C_{\text{ha1}} - C_{\text{ha3}}$	Intercept	-904.5	1517.0	-0.6 (0.583)	0.082	0.998	<0.01
	Large tree biomass	0.021	0.011	1.9 (0.124)	0.486		
	Large tree biomass ²	0.0001	0.0001	-0.5 (0.621)	0.0667		
	Small tree biomass	0.012	0.011	1.1 (0.337)	0.229		
	Small tree biomass ²	0.0001	0.0001	0.3 (0.757)	0.027		
	Conifer proportion	-945.3	1219.0	-0.8 (0.481)	0.131		
$C_{\text{ha1}} - C_{\text{ha4}}$	Intercept	-383.4	1795.0	-0.2 (0.841)	0.011	0.999	<0.01
	Large tree biomass	0.015	0.013	1.1 (0.325)	0.239		
	Large tree biomass ²	0.0001	0.0001	1.6 (0.191)	0.382		
	Small tree biomass	0.02	0.013	1.6 (0.197)	0.375		
	Small tree biomass ²	0.0001	0.0001	2.0 (0.117)	0.498		
	Conifer proportion	2681.0	1442.0	1.9 (0.137)	0.463		
$C_{\text{ha1}} - C_{\text{ha5}}$	Intercept	-383.4	1795.0	-0.2 (0.841)	0.011	0.889	0.01
	Large tree biomass	-0.019	0.013	-1.4 (0.227)	0.337		
	Large tree biomass ²	0.0001	0.0001	1.6 (0.191)	0.382		
	Small tree biomass	-0.013	0.013	-1.0 (0.369)	0.204		
	Small tree biomass ²	0.0001	0.0001	2.0 (0.117)	0.498		
	Conifer proportion	2681.0	1442.0	1.9 (0.137)	0.463		



633
 634 **Fig. A1.** Differences in 400-m² subplot-level carbon (C_{subplot}) stocks (measured in kg C subplot⁻¹) estimated using
 635 different wood carbon fraction (CF) assumptions. Subplot-level differences are calculated as the difference between
 636 C_{subplot1} (generated using species-specific wood CF data) vs. C_{subplot2} (generated assuming wood CFs for temperate
 637 biome trees specific to conifers and angiosperms); C_{subplot3} (generated assuming non-biome-specific wood CFs for
 638 conifers and angiosperms); C_{subplot4} (generated assuming a single IPCC default wood CF assumption); and C_{subplot5}
 639 (generated assuming a single 50% wood CF assumption). Red dotted line denotes differences between the two C
 640 estimation values of 0. Therefore i) all values above 0 indicate instances where species-specific wood CFs (C_{subplot1})
 641 are higher compared to estimates generated using generalized wood CF assumptions ($C_{\text{subplot2}}-C_{\text{subplot5}}$), and ii) all
 642 values below 0 indicate instances where species-specific wood CFs (C_{subplot1}) are lower compared to estimates
 643 generated using generalized wood CF assumptions ($C_{\text{subplot2}}-C_{\text{subplot5}}$). Open circles denote individual subplots
 644 ($n=368$ subplots total) and closed symbols denote mean differences for a given comparison (± 1 s.d.). Values here
 645 are presented visually in Fig. 3 and summarized in Table 2 in the main text.

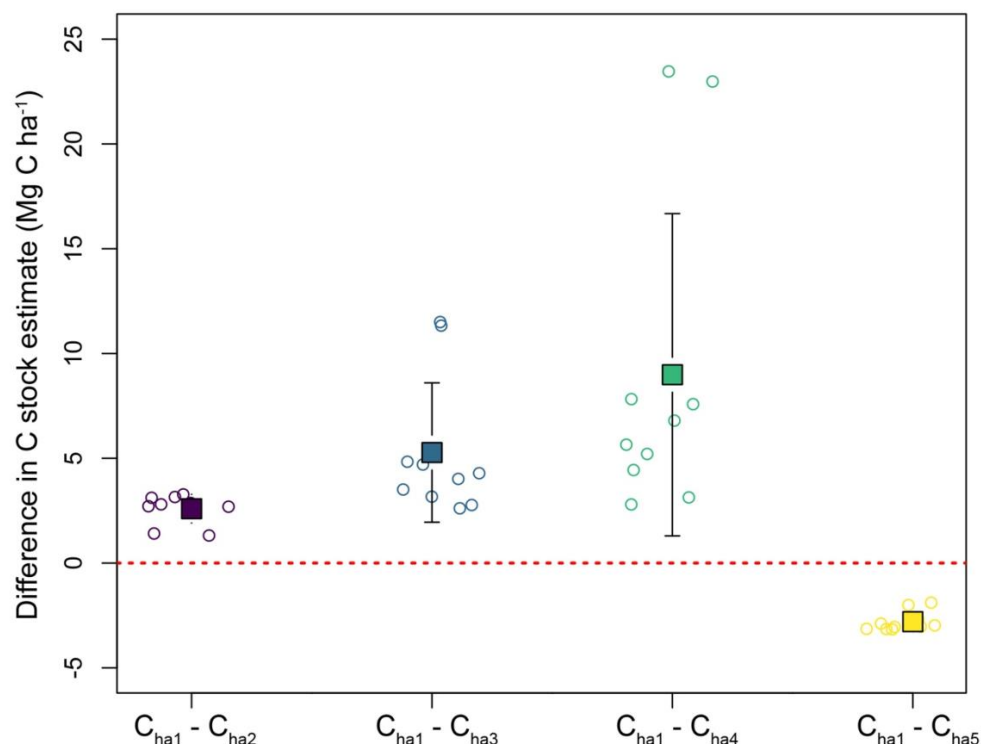


Fig. A2. Differences in per ha subplot-level carbon (C_{ha}) stocks (measured in Mg C ha^{-1}) estimated using different wood carbon fraction (CF) assumptions. Per ha-level differences are calculated as the difference between C_{ha1} (generated using species-specific wood CF data) vs. C_{ha2} (generated assuming wood CFs for temperate biome trees specific to conifers and angiosperms); C_{ha3} (generated assuming non-biome-specific wood CFs for conifers and angiosperms); C_{ha4} (generated assuming a single IPCC default wood CF assumption); and C_{ha5} (generated assuming a single 50% wood CF assumption). Red dotted line denotes differences between the two C estimation values of 0. Therefore i) all values above 0 indicate instances where species-specific wood CFs (C_{ha1}) are higher compared to estimates generated using generalized wood CF assumptions ($C_{ha2}-C_{ha5}$), and ii) all values below 0 indicate instances where species-specific wood CFs (C_{ha1}) are lower compared to estimates generated using generalized wood CF assumptions ($C_{ha2}-C_{ha5}$). Open circles denote individual ha of forest ($n=10$ individual ha total) and closed symbols denote mean differences for a given comparison (± 1 s.d.). Values here are presented visually in Fig. 4 and summarized in Table 2 in the main text.